

**Direct Monte Carlo Simulations of Hypersonic Low-Density
Flows about an ASTV Including Wake Structure**

V. K. Dogra

Vignon, Inc., Hampton, Virginia

and

J. N. Moss, R. G. Wilmoth, and J. M. Price

NASA Langley Research Center, Hampton, Virginia



Reprinted from *Rarefied Gas Dynamics: Space Science and Engineering*, edited by Bernie D. Shizgal and David P. Weaver, Vol. 160 of *Progress in Astronautics and Aeronautics*, AIAA, Washington, DC, ISBN 1-56347-081-0.

Direct Monte Carlo Simulations of Hypersonic Low-Density Flows About an ASTV Including Wake Structure

V. K. Dogra*

Vignam, Inc., Hampton, Virginia 23666

and

J. N. Moss,† R. G. Wilmoth,† and J. M. Price†

NASA Langley Research Center, Hampton, Virginia 23665

Abstract

Results of a numerical study concerning flow past a 70-deg blunted cone in hypersonic low-density flow environments are presented using the direct simulation Monte Carlo method. The flow conditions simulated are those that can be obtained in existing low-density hypersonic wind tunnels. Results indicate that a stable vortex forms in the near wake at and below a freestream Knudsen number (based on cone diameter) of 0.01 and the size of the vortex increases with decreasing Knudsen number. The base region of the flow remains in thermal nonequilibrium for all cases considered herein.

Nomenclature

A	= base area of cone, $\pi d^2/4$
C_D	= drag coefficient, $2D/\rho_\infty V_\infty^2 A$
C_H	= heat transfer coefficient, $2q/\rho_\infty V_\infty^3$
d	= base diameter
D	= drag
Kn	= Knudsen number, λ/d

Copyright © 1992 by the American Institute of Aeronautics and Astronautics, Inc. No copyright is asserted in the United States under Title 17, U.S. Code. The U.S. Government has a royalty-free license to exercise all rights under the copyright claimed herein for Governmental purposes. All other rights are reserved by the copyright owner.

*Research Engineer.

†Research Engineer, Space Systems Division.

M	= Mach number
p	= pressure
R	= radius
Re	= Reynolds number, $\rho V d / \mu$
Re_2	= total Reynolds number, $Re_\infty (\mu_\infty / \mu_o)$
s	= distance along the body surface measured from stagnation point
S	= speed ratio
T	= thermodynamic temperature
T_i	= translational kinetic temperature
u	= axial velocity
v	= radial velocity
V	= velocity
x	= axial distance from stagnation point measured along symmetry axis
$(x/d)_o$	= location of rear stagnation point
$(x/d)_1$	= location of wake stagnation point
y	= radial distance from symmetry axis
Δ	= size of the vortex, = $(x/d)_1 - (x/d)_o$
λ	= mean free path
μ	= dynamic viscosity
ρ	= density

Subscripts

a	= axial
c	= corner
n	= nose
$stag$	= forebody stagnation point values
r	= radial
w	= surface values
o	= stagnation chamber values
∞	= freestream values

Introduction

Aeroassisted Space Transfer Vehicles (ASTV) will have three primary components: aerobrake, payload compartment, and main propulsion unit. These vehicles will maneuver within the rarefied and generally undefined outer atmosphere rather than just passing through it. Recent studies¹⁻⁴ in the transitional flow regime of the aerothermal loads of various blunt bodies associated with current and projected ASTVs have focused mainly on the aerobrake. However, little is known about the wake structure of the aerobrake, which will interact with the payload compartment and main propulsion unit. The heating rate and aerodynamic forces that can result

from the interaction of the near wake with the payload compartment can influence significantly the size and shape of the afterbody configuration. There is a lack of experimental data for blunt body wake flows in the hypersonic rarefied flow regime. The structure of the near wake of an aerobrake in the continuum flow regime has been numerically studied recently,⁵ using the Navier-Stokes equations. Although the forebody may be in the continuum flow regime, the expansion into the wake region can produce large local Knudsen numbers. Consequently, it becomes imperative that the wake be investigated with an analysis capable of properly modeling the general features of low density-flows.

Recent direct simulation Monte Carlo (DSMC) simulations⁶ of rarefied hypersonic flows about spheres show that the calculated sphere drag agrees well with measured wind-tunnel values. These calculations also show that the wake is very rarefied, and that there are no vortices in the wake for freestream Knudsen numbers between 0.8 and 0.009. For similar flow conditions, Brewer's⁸ DSMC blunt body calculations also agree with these results. The Navier-Stokes calculations of Ref. 7 for similar flow conditions agree well with experimental drag but predict a steady vortex in the wake at a freestream Knudsen number value of 0.009. Such discrepancies highlight the importance of using a particle simulation method such as DSMC to establish a database for isolating the features of wake flows under conditions where rarefaction effects are significant. Furthermore, parallel studies using Navier-Stokes and DSMC simulations can establish the bounds for which continuum methods are appropriate.

In the present paper, the DSMC method^{9,10} has been used to simulate the low-density axisymmetric flow of nitrogen about a 70-deg half-angle, blunted cone with a base diameter of 5 cm (a wind-tunnel model of the Viking lander aeroshell¹¹). This model provides a realistic generic ASTV configuration for investigating the wake structure.

Conditions for Calculations

The flow conditions considered are attainable in the SR3 tunnel at Centre National de la Recherche Scientifique (CNRS¹²), and are listed in Table 1. The model size selected is such that it can be tested in existing low-density hypersonic wind tunnels (Table 2). The surface temperature is assumed to be constant at 300 K, and the gas-surface interaction model is diffuse with full thermal accommodation. Because of the relatively low total temperature, the DSMC simulations model the nitrogen flow as a nonreacting gas with energy exchange between rotational and translational modes. The freestream parameters along with selected results are summarized in Table 2.

Table 1 Wind-tunnel^a conditions for flow about a blunted 70-deg cone^b

Case	T_0 , K	P_0 , bar	M_∞	$\rho_\infty \times 10^5$ kg/m ³	V_∞ , m/s	T_∞ , K	Kn_∞
1	1099	3.5	20.2	1.73	1502	13.3	0.0317
2	1100	9.3	19.7	5.19	1502	14.0	0.0107
3	1299	125.5	20.6	46.65	1633	15.0	0.0012

^aFreestream conditions are those that can be obtained in the SR3 wind tunnel (Meudon, France). The test gas is nitrogen.

^bSurface conditions: $T_w = 300$ K, diffuse with full thermal accommodation.

Table 2 Flow parameters and surface quantities^a

Case	Re_∞	Re_2	λ_∞ mm	S_∞	CD	CH_{stag}	Δ
1	768	28.0	1.588	16.9	1.61	0.366	0.00
2	2,220	84.1	0.535	16.5	1.54	0.213	0.19
3	20,600	725.7	0.061	17.3	1.54	0.0965	0.75

^aModel diameter: $d = 4.95$ cm, nose radius: $R_n = 1.25$ cm, corner radius: $R_c = 0.036$ cm.

Results and Discussion

Attention is focused on the flowfield structure of the forebody and the wake regions, but with major emphasis on the wake. In addition, surface quantities and drag resulting from low-density simulations are presented for the flow about a 70-deg blunted cone.

Forebody Flow Structure

Figure 1 shows the density contours for case 2. Near the stagnation point, a substantial density increase occurs for all three cases considered. This is characteristic of hypersonic flows about cold blunt surfaces. It has been observed from the density contours for the two most rarefied cases that the density rises gradually as the flow approaches the body, indicating the diffuse nature of the shock wave that is characteristic of highly rarefied flows. However, for case 3, where $Kn_\infty = 0.001$, the density contours show a rapid rise of density as the flow approaches the body, indicating the formation of a thick shock wave. In addition, the calculated results indicate (not shown) that the Mach 1 contour approaches the body surface at the aft corner, and the forebody is enveloped in a rather thick subsonic layer.

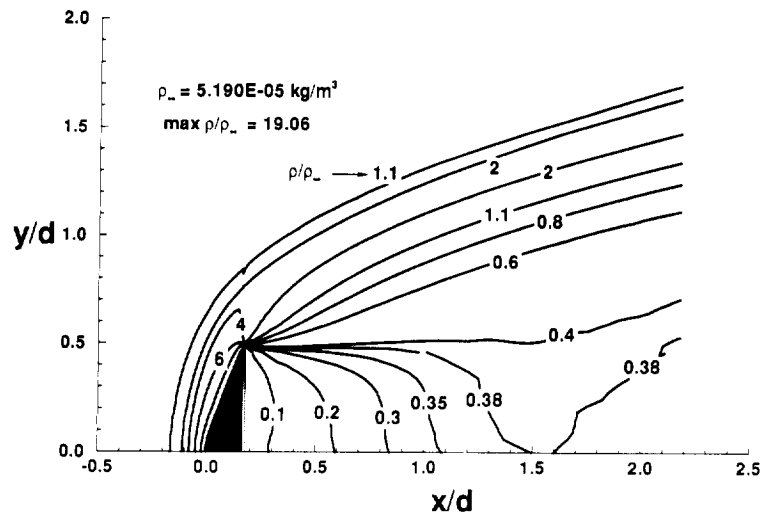


Fig. 1 Nondimensional density contours (Case 2, $M_\infty = 19.7$, $Kn_\infty = 0.0107$, $Re_\infty = 2220$).

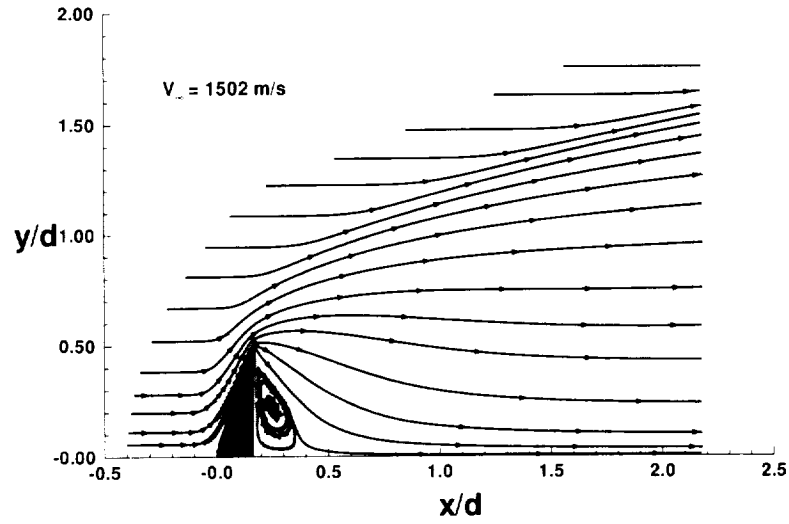


Fig. 2 Streamlines (Case 2, $M_\infty = 19.7$, $Kn_\infty = 0.0107$, $Re_\infty = 2220$).

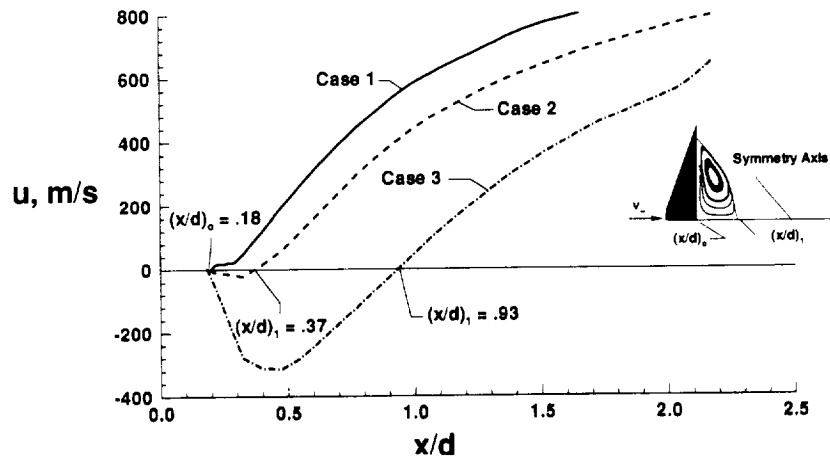


Fig. 3 Axial velocity along the symmetry axis of the wake.

Wake Structure

The density in the near wake for all three cases is less than 40 % of the freestream value. The density even drops below 10 % of the freestream value in a region near the base, and this zone of very low density increases in size as the freestream Knudsen number increases. It has been also observed from these calculations that there is a substantial amount of thermal nonequilibrium in the entire wake region for cases 1 and 2. For case 3, most of the wake region is in thermal equilibrium. There is a small region near the base where the flow remains in thermal nonequilibrium. In addition to these thermal nonequilibrium effects, a substantial portion of the wake flow in the base region is subsonic, and the extent of this subsonic region increases with decreasing freestream Knudsen number.

The streamline plots show that the flow is attached to the surface, and there is no evidence of flow separation for case 1. This is expected because of the rarefied flow condition ($Kn_\infty = 0.0317$ and $Re_\infty = 768$). However, for cases 2 and 3, the flow separates beyond the corner on the base of the body and a stable vortex develops in the base region of the wake (shown in Fig. 2 for case 2 only). It can also be inferred from these results that the separation point moves closer to the body corner with decreasing freestream Knudsen number.

The wake stagnation point is generally defined for separated flows as the location of a point in the wake where the flow reattaches and the flow velocity is zero. For axisymmetric separated flow, this point lies on the symmetry axis of the wake where the axial velocity is zero. The effect of rarefaction on the location of the wake stagnation point is shown in Fig. 3. The wake stagnation point moves toward the rear stagnation point with increasing freestream Knudsen number and finally coincides with the rear stagnation point for attached flow. Therefore, the size of the vortex (Δ) increases with decreasing rarefaction. The axial and radial components of translational temperature along the wake symmetry axis for cases 2 and 3 are shown in Fig. 4. The translational thermal nonequilibrium exists all along the symmetry axis for case 2. For case 3, the flow along the wake symmetry axis is in translational equilibrium downstream of the wake stagnation point, and the translational temperature attains the highest value at the wake stagnation point (Fig. 4).

Figure 5 presents the axial velocity variation in the radial direction at three different axial locations in the wake for case 3. These results show that the shear-layer thickness changes very gradually with distance downstream of the base, and that the leading-edge bow shock wave gradually becomes weak as the flow moves downstream in the wake. In addition, the lip expansion fan diffuses in the streamwise direction and there is no indication of any distinct wake compression wave. For the more rarefied cases, it is observed that there are no distinct wake flow features, as shown in Fig. 5 for case 3. The lip expansion fan merges gradually with the shear layer and bow shock as the freestream Knudsen number increases.

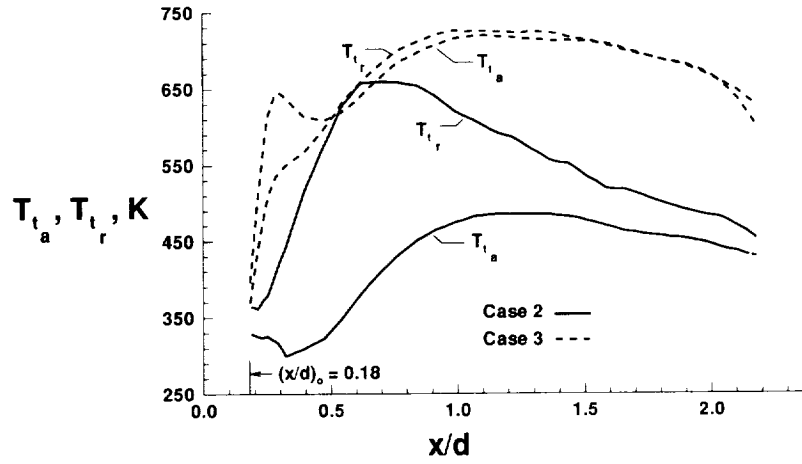


Fig. 4 Axial and radial translational kinetic temperatures along the symmetry axis of the wake.

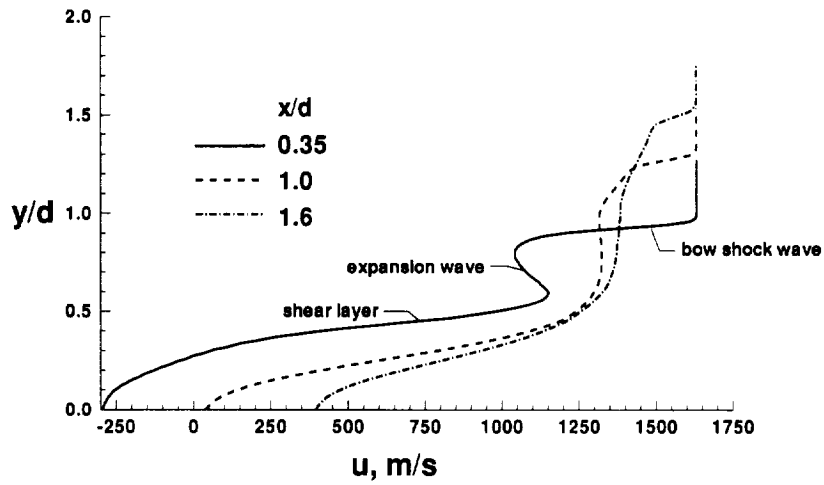


Fig. 5 Axial velocity profiles normal to the symmetry axis of the wake.

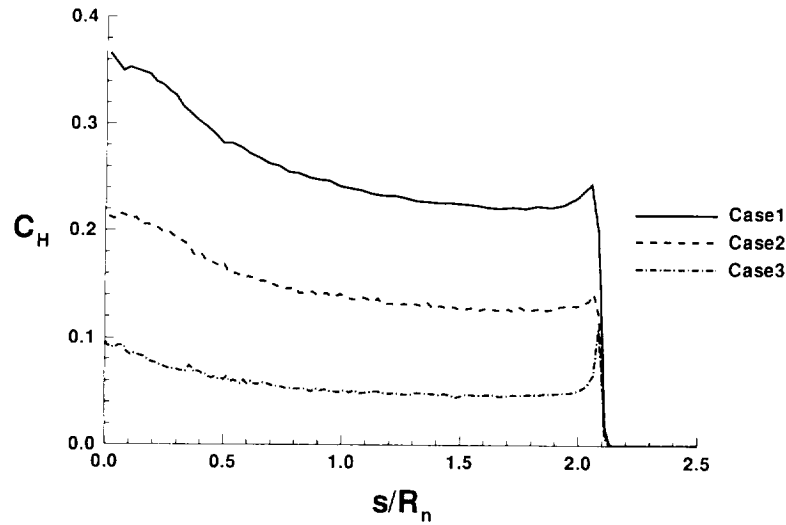


Fig. 6 Effect of rarefaction on the surface heat transfer.

Surface Quantities

The surface heat transfer coefficient is presented in Fig. 6 for all three cases. The results are shown as a function of the nondimensional distance (s/R_n) along the surface measured from the forebody stagnation point. The expansion of the flow about the aft corner for case 3 causes the maximum heat transfer at that point, rather than at the stagnation point (Fig. 6). The present calculations also show that the surface pressure is not very sensitive to rarefaction since the forebody is enveloped with a fairly thick subsonic layer. The surface quantities on the base surface are very small compared with those on the forebody surface for all three cases.

Conclusion

Direct simulation Monte Carlo simulations of blunt body flows have been performed for flow conditions that can be achieved in existing low-density wind tunnels. For the range of the Knudsen numbers considered (0.03-0.001), the calculated results show that a stable vortex exists in the base region of the wake for freestream Knudsen numbers between 0.01 and 0.001, and the size of the vortex increases with decreasing freestream Knudsen number. There is no formation of a lip separation shock or a distinct wake shock at these rarefied conditions. This is contrary to the behavior observed for blunt body flows at continuum hypersonic conditions.

References

- ¹Moss, J. N. and Bird, G. A., "Direct Simulations of Transitional Flow for Hypersonic Reentry Conditions," *Thermal Design of Aeroassisted Orbital Transfer Vehicles, Progress in Astronautics and Aeronautics: Vol. 96*, edited by H.F. Nelson, AIAA, New York, 1985, pp. 113-139.
- ²Dogra, V. K., Moss, J. N., and Simmonds, A. L., "Direct Simulation of Aerothermal Loads for an Aeroassist Flight Experiment Vehicle," AIAA Paper 87-1546, June 1987.
- ³Celenligil, M. C., Moss, J. N., and Blanchard, R. C., "Three-Dimensional Rarefied Flow Simulations for the Aeroassist Flight Experiment Vehicle," *AIAA Journal*, Vol. 29, Jan. 1991, pp. 52-57.
- ⁴Feiereisen, W. J. and McDonald, J. D., "Three-Dimensional Discrete Particle Simulation of an AOTV," AIAA Paper 89-1711, June 1989.
- ⁵Gnoffo, P. A., Price, J. M., and Braun, R. D., "Computation of Near-Wake, Aerobrake Flowfields," *Journal of Spacecraft and Rockets*, Vol. 29, No. 2, Mar.-Apr. 1992, pp. 182-189.
- ⁶Dogra, V. K., Moss, J. N., Wilmoth, R. G., and Price, J. M., "Hypersonic Rarefied Flow Past Spheres Including Wake Structure," AIAA Paper 92-0495, Jan. 1992.
- ⁷Jain, A. C. and Dahm, W. K., "Hypersonic Merged Layer Blunt Body Flows with Wakes," *Proceedings of the 17th International Symposium on Rarefied Gas Dynamics*, 1990, pp. 578-587.
- ⁸Brewer, E. B., Private Communication, NASA-Marshall Space Flight Center, Huntsville, Al., 1991-1992.
- ⁹Bird, G. A., *Molecular Gas Dynamics*, Clarendon, Oxford, England, 1976.
- ¹⁰Bird, G. A., "Monte-Carlo Simulation in an Engineering Context," *Progress in Astronautics and Aeronautics: Rarefied Gas Dynamics, Part I, Vol.74*, edited by S. S. Fisher, AIAA, New York, 1981, pp. 239-255.
- ¹¹Blanchard, R. C. and Walberg, G. D., "Determination of the Hypersonic Continuum/ Rarefied Flow Drag Coefficient of the Viking Lander Capsule Aeroshell from Flight Data," NASA TP-1793, Dec. 1980.
- ¹²Allegre, J., "The SR3 Low Density Wind-tunnel. Facility Capabilities and Research Development," AIAA Paper 92-3972, July 1992.

